INVESTIGATION OF ELASTOMERIC PAD ATTENUATION OF HAND-TRANSMITTED VIBRATION

KO YING HAO

UNIVERSITI SAINS MALAYSIA

2008

INVESTIGATION OF ELASTOMERIC PAD ATTENUATION OF HAND-TRANSMITTED VIBRATION

by

KO YING HAO

Thesis submitted in fulfillment of the requirements for the degree of Master of Science

JUNE 2008

ACKNOWLEDGEMENTS

First of all, I would also like to express my sincere gratitude to my research supervisor, Assoc. Prof. Dr. Zaidi bin Mohd Ripin. The successful completion of this thesis depended on his useful ideas and constant encouragement throughout the entire study.

Gratitude extended to my co-supervisor Dr. Inzarul Faisham Abd Rahim for his sincerely guidance. Thanks also go to Mr. Wan Muhamad Amri Wan Ali and Baharum Awang, technician of The Vibration Lab and Material lab, for their help and assistance.

I would like to forward special thanks to my fellow friends Mr. Ezral, Mr. Lim Mook Tzeng, Mr. Rosmaini, Mr. Khairul Anuar, Mr. Chuah Han Guan and Ms. Wong Wai Chi for their moral supports. Thanks are also to all students and staff of Universiti Sains Malaysia, those who helped me either directly or indirectly in completing my research.

Besides, I am gratitude to Universiti Sains Malaysia for awarding me the GRADUTE ASSISTANT SCHEME scholarship which relieved me of financial insecurity.

Furthermore, I would like to express my deepest gratitude to my family for their love, support and encouragement. Last but not least, I would like to thank my fiancé, Mr. Roland Voon Gah Seng, whose support contributed to the completion of this thesis.

KO YING HAO

June 2008

TABLE OF CONTENTS

LIST OF TABLES

LIST OF FIGURES

LIST OF SYMBOLS

Symbol	Description	Unit
A	Amplitude	-
A_e	Elastomeric pad's effective load area	m^2
$A(8)$	Daily vibration exposure based on reference period of 8 hours	ms^{-2}
$A(4)$	Daily vibration exposure based on reference period of 4 hours	ms^{-2}
a_j	RMS acceleration corresponding to the j^{th} 1/3 octave band	ms^{-2} (rms)
a_{hv}	vibration total value	ms^{-2}
a_{hwx}	overall weighted RMS acceleration at x axis	ms^{-2}
a_{hwy}	overall weighted RMS acceleration at y axis	ms^{-2}
a_{hwz}	overall weighted RMS acceleration at z axis	ms^{-2}
a_w	overall weighted RMS acceleration	$ms^{-2}rms$
$[C]$	Damping matrix	-
$[C]_{el}$	Damping matrix of coupled elastomeric pad and hand-arm model	-
$[C]_{fd}$	Damping matrix of coupled flow divider and hand-arm model	-
C_e	Damping of elastomeric pad	Ns/m
C_{eff}	Effective damping of elastomeric pad	Ns/m
$\{C_i\}$	Forcing damping vector	-
$\{C_i\}_{el}$	Forcing damping vector of coupled elastomeric pad and hand-arm model	-
$\{C_i\}_{fd}$	Forcing damping vector of coupled flow divider and hand-arm model	-
C_{t1}	Rotational damping property at upper arm at shoulder joint (pitch direction)	Nms/rad
C_{t2}	Rotational damping property at forearm at elbow joint (pitch direction)	Nms/rad
C_0	Damping property at hand-handle interface	Ns/m

C_1	Damping property at hand and forearm at wrist joint	Ns/m
C_2	Damping property at forearm at elbow joint	Ns/m
C_3	Damping property at upper arm at shoulder joint (longitudinal direction)	Ns/m
C_4	Damping property at upper arm at shoulder joint (vertical direction)	Ns/m
C^*	Damping of flow divider	Ns/m
E_s	Shear modulus	MPa
$E(\Upsilon)$	error function	-
$F(j\omega)$	Complex quantity of excitation force	N
i	Imaginary part	-
J_c	Mass moment inertia of upper arm	kgm^2
$[K]$	Stiffness matrix	-
$[K]_{el}$	Stiffness matrix for coupled elastomeric pad and hand-arm model	-
$[K]_{fd}$	Stiffness matrix for coupled flow divider and hand-arm model	-
K_e	Stiffness of elastomeric pad	Nm^{-1}
K_{eff}	Effective stiffness of elastomeric pad	Nm^{-1}
K_s	Shear stiffness	Nm^{-1}
$\{K_i\}$	Forcing damping vector	-
$\{K_i\}_{el}$	Forcing damping vector of coupled elastomeric pad and hand-arm model	-
$\{K_i\}_{fd}$	Forcing damping vector of coupled flow divider and hand-arm model	-
k_j	weighting frequency factor	-
K_{t1}	Rotational stiffness property at upper arm at shoulder joint (pitch direction)	Nm/rad
K_{t2}	Rotational stiffness property at forearm at elbow joint (pitch direction)	Nm/rad
K_0	Stiffness property at hand-handle interface	Nm^{-1}

K_1	Stiffness property at hand and forearm at wrist joint	Nm^{-1}
K_2	Stiffness property at forearm at elbow joint	Nm^{-1}
K_3	Stiffness property at upper arm at shoulder joint (longitudinal direction)	Nm^{-1}
K_4	Stiffness property at upper arm at shoulder joint (vertical direction)	Nm^{-1}
K^*	Stiffness of flow divider	Nm^{-1}
L	Length of upper arm	m
L	Lower bound of design parameter	
L_{cg}	Length of upper arm due to center of gravity	m
ℓ	Length of elastomeric pad	m
$[M]$	Mass matrix	-
$[M]_{el}$	Mass matrix of coupled elastomeric pad and hand-arm model	-
$[M]_{fd}$	Mass matrix of coupled flow divider and hand-arm model	-
m_1	Mass of hand	kg
m_2	Mass of forearm	kg
m_3	Mass of upper arm	kg
m^*	Mass of flow divider	kg
N	Number of elastomeric pad	-
n	Number of cycles	-
p	number of 1/3 octave band used	-
r	number of location where acceleration transmissibility are measured	-
$S_h(\omega)$	RMS acceleration input spectrum	ms^{-2}
$\{S_o(\omega)\}$	RMS acceleration output spectrum	ms^{-2}
$\{S_{oh}(\omega)\}$	RMS acceleration response spectrum for hand	ms^{-2}
$\{S_{of}(\omega)\}$	RMS acceleration response spectrum for forearm	ms^{-2}
$\{S_{ou}(\omega)\}$	RMS acceleration response spectrum for upper arm	ms^{-2}

$\{S_o(\omega)\}_{el}$	RMS acceleration response spectrum of coupled elastomeric pad and hand-arm model	ms^{-2}
$\{S_o(\omega)\}_{fd}$	RMS acceleration response spectrum of coupled flow divider and hand-arm model	ms^{-2}
$\left\{\frac{\ddot{U}}{\ddot{Z}_0}(j\omega)\right\}_{el}$	Complex acceleration transmissibility function of coupled elastomeric pad and hand-arm model	ms^{-2}
$\left\{\frac{\ddot{U}_1}{\ddot{Z}_0}(j\omega)\right\}_{el}$	Complex acceleration transmissibility response function for hand when coupled with elastomeric pad	ms^{-2}
$\left\{\frac{\ddot{U}_2}{\ddot{Z}_0}(j\omega)\right\}_{el}$	Complex acceleration transmissibility response function for forearm when coupled with elastomeric pad	ms^{-2}
$\left\{\frac{\ddot{U}_3}{\ddot{Z}_0}(j\omega)\right\}_{el}$	Complex acceleration transmissibility response function for upper arm when coupled with elastomeric pad	ms^{-2}
$\left\{\frac{\ddot{U}}{\ddot{Z}_0}(j\omega)\right\}_{fd}$	Complex acceleration transmissibility function of coupled flow divider and hand-arm model	ms^{-2}
$\left\{\frac{\ddot{U}_1}{\ddot{Z}_0}(j\omega)\right\}_{fd}$	Complex acceleration transmissibility response function for hand when coupled with flow divider	ms^{-2}
$\left\{\frac{\ddot{U}_2}{\ddot{Z}_0}(j\omega)\right\}_{fd}$	Complex acceleration transmissibility response function for forearm when coupled with flow divider	ms^{-2}
$\left\{\frac{\ddot{U}_3}{\ddot{Z}_0}(j\omega)\right\}_{fd}$	Complex acceleration transmissibility response function for upper arm when coupled with flow divider	ms^{-2}
s	number of discrete frequencies considered	-
T	Period	s
$T_{cj}(\omega_i)$	Computed acceleration transmissibility of location r derived from hand arm model	-
$T_{mj}(\omega_i)$	Corresponding measured acceleration transmissibility	-
$T(j\omega)$	Complex function of vibration transmissibility	-
T_0	Reference duration of eight hours	h
t	Time	s
t_e	Elastomeric pad's thickness	m
t_o	Arbitrary instant	s

T_v	daily duration of exposure to the vibration magnitude	ms^{-2}
U	Upper bound of design parameter	-
$\{U\}$	(5×1) vector of generalized displacement coordinates	-
$\{U\}_{el}$	(5×1) vector of generalized displacement coordinates of coupled elastomeric pad and hand-arm model	-
$\{U\}_{fd}$	(6×1) vector of generalized displacement coordinates of coupled flow divider and hand-arm model	-
w	Width of elastomeric pad	m
X_3	vertical motion of the elbow joint	-
$\dot{X}(j\omega)$	Complex quantity of resulting vibration velocity	ms^{-1}
$X_i(j\omega)$	Complex response of forcing displacement	m
$\dot{X}_i(j\omega)$	Complex response of forcing velocity	ms^{-1}
$\ddot{X}_i(j\omega)$	Complex response of forcing acceleration	ms^{-2}
$X_0(j\omega)$	Complex response of resulting displacement	m
$\dot{X}_o(j\omega)$	Complex response of resulting velocity	ms^{-1}
$\ddot{X}_o(j\omega)$	Complex response of resulting acceleration	ms^{-2}
Z_3	Longitudinal motion of upper arm	-
$Z(j\omega)$	Complex quantity of DPMI	-
η	Loss factor	-
ϕ	Phase different	rad
ω	Excitation frequency	rad
ω_j^*	Complex j^{th} natural frequency	rad
$\omega_j^{'}$	Real part of the complex j^{th} natural frequency	rad
$\omega_j^{''}$	Imaginary part of the complex j^{th} natural frequency	rad
Δt	Different between two distinct time	s
π	Pi	-
θ	Pitch direction	-

θ_3	Pitch rotation of the upper arm with respect to the elbow joint	-
$\left[\frac{\ddot{U}_1}{\ddot{Z}_o}\right]$	Acceleration transmissibility for hand	-
$\left[\frac{\ddot{U}_2}{\ddot{Z}_o}\right]$	Acceleration transmissibility for forearm	-
$\left[\frac{\ddot{U}_3}{\ddot{Z}_o}\right]$	Acceleration transmissibility for upper arm	-
Υ	design parameters	-
$\frac{X_o}{X_i}(j\omega)$	Displacement transmissibility	-
$\frac{\dot{X}_o}{\dot{X}_i}(j\omega)$	Velocity transmissibility	-
$\frac{\ddot{X}_o}{\ddot{X}_i}(j\omega)$	Acceleration transmissibility	-

LIST OF NOTATIONS

Symbol	Description
CTS	Carpal tunnel syndrome
DOF	Degree of freedom
EAV	Exposure action value
ELV	Exposure limit value
EU	European union
HAVs	Hand-arm vibration syndrome
HTV	Hand- transmitted vibration
ISO	International Standard Organization
DPMI	Driving-point mechanical impedance

LIST OF APPENDICES

LIST OF PUBLICATIONS

KAJIAN KE ATAS KESAN LAPIK ELASTOMER BAGI MENGURANGKAN GETARAN DIHANTAR KE TANGAN

ABSTRAK

Pekerja yang menggunakan peralatan berkuasa dalam pekerjaan terdedah kepada getaran dihantar ke tangan. Pendedahan yang melampau terhadap getaran tersebut akan menyebabkan beberapa kesan negatif di bahagian tangan. Kesan ini dikenali sebagai sindrom getaran tangan (HAVS). Untuk menilai kesan lapik elastomer dalam mengurangkan getaran yang dihantar ke tangan, satu model matematik yang menggabungkan lapik elastomer dengan model tangan (dicadangkan oleh Cherian et al. (1996)) telah dibentuk. Sebagai langkah pertama, kesan lapik elastomer telah dikaji secara analisis. Dalam kajian optimal bagi lapik elastomer, ianya menunjukan parameter yang optimal bagi lebar, panjang dan nombor pelapisan adalah bersamaan dengan $50mm$, $50mm$, 3. Dengan menggunakan reka bentuk lapik elastomer yang optimal, keseluruhan pecutan RMS dapat dikira dan didapati keseluruhan pecutan RMS di bahagian tangan, lengan bawah dan lengan atas telah dikurangkan sebanyak 56%, 24% dan 24%. Dalam erti lain, lapik elastomer ini dapat mengatasi kelemahan pembahagi aliran yang dicadangkan oleh Cherian et al. (1996), yang meningkatkan paras getaran di bahagian lengan bawah dan lengan atas tangan. Parameter bagi model tangan diperolehi dengan mengukur keboleh-sebaran getaran dan data antropometrik. Ciri-ciri tindak balas bagi model gabungan lapik elastomer dengan tangan dibandingkan dari segi analisis dan ujikaji untuk mengesahkan keberkesanan lapik elastomer dalam mengurangkan getaran disampaikan ke tangan. Keputusan menunjukan keseluruhan pecutan RMS yang diperolehi secara ujikaji adalah hampir sama dengan keputusan yang didapati secara analisis, dengan peratus ketidak tepatan dari 2% ke 4% (tindak balas tangan) dan dari 3% ke 9% (tindak balas tangan dengan lapik elastomer). Dengan menggunakan lapik elastomer, pendedahan getaran seharian, A(8) menunjukan pengurangan paras getaran dari $1.1 - 1.4\, ms^{-2}$ ke $0.2 - 0.6\, ms^{-2}$. Kesimpulannya, lapik elastomer mampu mengurangkan paras getaran yang disampaikan ke tangan dengan berkesan.

INVESTIGATION OF ELASTOMERIC PAD ATTENUATION OF HAND-TRANSMITTED VIBRATION

ABSTRACT

Workers operating hand-held power tools are exposed to hand-transmitted vibration in their occupation. Extensive exposure of hand-transmitted vibration can lead to several disorders in hand-arm, known as hand-arm vibration syndrome (HAVs). In order to evaluate the effect of an elastomeric pad on reducing the hand-transmitted vibration, a coupled elastomeric pad and hand-arm model is formed based on an earlier model by Cherian et al. (1996). In the first stage, the effect of elastomeric pad was analysed using the model. The elastomeric pad with the optimum parameters of $50mm$ for both the width and length and number layer of 3, resulted in the calculated overall weighted RMS acceleration reduction for the hand, forearm and upper arm of 56%, 24% and 24% respectively. The elastomeric pad overcame the short coming of the flow divider as proposed by Cherian et al. (1995), which increases vibration of the forearm and upper arm. For experimental validation, parameters of a hand-arm model are derived using vibration transmissibility test and anthropometric data. The response characteristics of the coupled elastomeric pad-hand-arm model are compared analytically and experimentally to hand-arm model to demonstrate the potential of elastomeric pad in attenuating hand-transmitted vibration. The experimental results showed that the measured overall weighted RMS accelerations correlate well with those computed, with the difference percentage of 2% to 4% (hand response) and 3% to 9% (hand response with pad). Furthermore, with the use of elastomeric pad, the daily vibration exposure, A(8) show reduced vibration level from $1.1 \sim 1.4\, ms^{-2}$ to $0.2 \sim 0.6\, ms^{-2}$. It can be concluded that the elastomeric pad attenuated the acceleration level of hand-transmitted vibration effectively.

CHAPTER 1
INTRODUCTION

1.0 Overview

In this chapter, a brief introduction of the thesis is presented. The chapter also discusses the objectives, motivation behind the research and highlights the contributions of the research. Finally, the chapter will describe the thesis outline.

1.1 Brief Introduction

The invention of hand-held power tools is important in various occupations, in agricultural, construction, mining, dental and medical work. Examples of hand-held power tools are jack hammers, grinders, grass trimmers and orbital sanders. These hand-held power tools expose workers to hand-transmitted vibration (HTV). Extensive exposure of hand-transmitted vibration may lead to a series of vibration-induced disorders in the vascular and non-vascular structures in human hand and arm. Both types of disorders are jointly referred to as hand-arm vibration syndrome or HAVs (Mansfield, 2005).

Hand-arm vibration syndrome (HAVs) is a health risk which needs to be highlighted among workers who use hand-held power tools. In 1911, Loriga reported the first document of the relationship between exposure of hand-transmitted vibration and HAVs (Bylund, 2004). From then on, great efforts have been made by researchers from different fields (medical, epidemiological, ergonomic and bio-engineering) to understand, evaluate, and overcome this issue.

To standardized the measurement of hand-transmitted vibration exposure, ISO 5349 (2001) has provided the relevant guideline. To evaluate health risk assessment of hand-arm vibration syndrome (HAVs), the European Union (2005) has stated the exposure action value (EAV) of $2.5ms^{-2}$ and exposure limit value (ELV) of $5.0ms^{-2}$ for daily vibration exposure

A(8). In the reported epidemiological studies, the averaged vibration levels for rock drill, pneumatic jackleg drill and orbital sander are $20ms^{-2}$, $25ms^{-2}$ and $7ms^{-2}$ respectively (Niekerk et al., 1998; Oddo et al., 2004; Cherian et al., 1996). These vibration levels are above the exposure action value of $2.5ms^{-2}$ and exposure limit value of $5.0ms^{-2}$. Hence, the employers are required to take further action on this.

Moreover, due to the desire to improve the understanding of vibration-transmitted characteristics of human hand-arm, many analytical hand-arm models have been developed since 1972. Most of these models are derived based on mechanical impedance biodynamic response functions, hence do not describe the dynamics of the musculoskeletal structure of human hand-arm (Aldien et al., 2006; Cherian et al., 1996).These models vary from single degree-of-freedom (SDOF) to multiple degrees-of freedom systems (MDOF). Rakheja et al. (2002) made a comparison among these types of models to evaluate their suitability in realizing a mechanical simulator or assessment of dynamic behaviors of the coupled hand-tool system. The results showed that most of these models cannot be applied for the development of mechanical hand-arm simulation (Rakheja et al., 2002) and did not adequately represent the biomechanical properties of the hand-arm system (Dong et al., 2005).

The human hand-arm is a highly complex, non-homogeneous continuous system. It is comprised of viscoelastic properties of muscles and bones. Thus, an analytical representation of human hand-arm model must be able to characterize the viscous elastic and inertia properties of the hand-arm (Cherian et al., 1996). For these reasons, the five degrees-of-freedom (5DOF) analytical model proposed by Cherian et al. (1996), which is derived based on vibration transmissibility biodynamic response function and capable of representing hand-arm's viscous, elastic and inertia properties, was selected as the hand-arm model in this study.

Over the past two decades, ergonomic and bio-engineering researchers have been contributing to the reduction of hand-transmitted vibration from hand-held power tools. The power tools have been redesigned to incorporate anti-vibration devices (either vibration absorption or vibration isolation) and also to include ergonomic considerations (Tudor, 1996; Lin et al, 2005). Cherian et al. (1996) have proposed a 0.5 kg flow divider (a kind of vibration absorber) attached to the hand-arm model. The resulting calculated overall weighted RMS acceleration of the hand decreases by 22%, while the forearm and the upper arm increase by 13% and 10% respectively. This is due to the characteristic of vibration absorber. Although it tends to absorb vibration at the connection point, it increases vibration at other points (Steffen & Rade, 2002).

The idea of combined vibration absorption and isolation principles on an electro-pneumatic hammer's handle has been proposed by Golysheva et al. (2004), and showed significant reduction of hand-transmitted vibration. However, the use of a vibration absorber on hand-arm model is not an ideal concept. This is due to the fact that the human hand-arm is highly damped system (Rakheja et al., 2002), hence additional vibration absorption at the hand-arm does not make sense. Furthermore, it causes some increase in forearm and elbow acceleration (Cherian et al., 1996) and the additional mass on the hand is inconvenient.

The use of vibration isolation, especially made of elastomeric material, to reduce vibration transmissibility in structures is well known. Elastomeric materials have been used as anti-vibration glove, vibration isolators in motor and engine (Dimarogonas, 1996; Oddo, 2004).

In this work, a vibration isolator made of elastomeric material in the form of an elastomeric pad is investigated. The effectiveness of elastomeric pad on attenuation of vibrations to the hand is evaluated analytically, compared and validated with experiments.

1.2 Motivation of the work

The evaluation of vibration-attenuation mechanisms based on either mechanical impedance or vibration transmission biodynamic response function of the hand-arm model, have rarely been studied. Furthermore, there has been no further work reported since Cherian et al. (1996) proposed the vibration transmissibility based hand-arm model. Moreover, their principle of introducing vibration absorption on hand-arm is not ideal and can be further improved. These reasons have motivated this work.

1.3 Objectives

In this work, there are three objectives to be achieved:

- To develop an elastomeric pad and hand-arm model.
- To compare the effectiveness of elastomeric pad with flow divider (Cherian et al., 1996).
- To investigate the effect of elastomeric pad on attenuation of hand-transmitted vibration analytically and experimentally.

1.4 Contributions

This section lists the contributions in the overall research.

- A mathematical model of coupled elastomeric pad and hand-arm model was formed.
- The effect of elastomeric pad in reducing hand-transmitted vibration has been explored analytically and experimentally.

1.5 Thesis outlines

The thesis is presented in five chapters which include the introduction, literature review, methodology, results and discussion and finally conclusions. The first chapter gives a brief introduction of the thesis. The objectives, motivation and contributions of the project are also presented in this chapter. In Chapter Two, a literature survey regarding health risks

of hand-arm vibration syndrome (HAVs), the standards for measurement and evaluation of hand-transmitted vibration, epidemiological studies on hand-arm vibration, review of the biodynamic models and mitigation of hand-transmitted vibration is presented. Chapter Three describes the methodology to achieve the thesis objectives. Results are presented and discussed in Chapter Four. Finally, the thesis ends with conclusions in Chapter Five.

CHAPTER 2
LITERATURE REVIEW

2.0 Overview

Prolonged use of hand-held power tools increases the risks of hand-arm vibration syndrome (HAVs). Owing to this, over the years, researchers from different fields have exerted effort to solve this problem. Researchers from biomedical field have studied the health risks of HAVs. International organizations have adopted on standards and guidelines for health risk assessment. Occupation health researchers have performed research on the epidemiologic of HAVs. Moreover, biomechanical researchers have found the ways to evaluate the vibration characteristic of human hand-arm system, vibration reduction and ergonomic design of more comfortable power tools.

Hence, literature reviews for five main scopes of the thesis are presented in this section. The scopes covered are as below:

- Health risks of hand-arm vibration syndrome (HAVs)
- Standards for measurement and evaluation of hand-transmitted vibration
- Epidemiological study of hand-arm vibration
- Review of biodynamic models of human hand-arm
- Mitigation of hand-transmitted vibration

2.1 Health risks of hand-arm vibration syndrome (HAVs)

By definition, hand-arm vibration syndrome (HAVs) is the combined disorders in the vascular and nonvascular system of the hand, due to prolonged exposure to hand-transmitted vibration from powered tools (Mansfield, 2005; Bovenzi, 1998).

The vascular aspect on hand-arm vibration syndrome (HAVs) is characterized by Secondary Raynaud's Disease (Bovenzi, 1998; Fridén, 2001; Stoyneva et al., 2003;

Mansfield, 2005). Characteristically, there are white and pale signs on fingers or commonly known as Vibration White Finger (VWF). Initially, there are episodes of blanching on the fingers, if vibration continues, the fingers turn red and are often painful. In the worst case, the fingers are irreversibly damaged (EU, 2005).

The nonvascular aspects of HAVs are represented by neurological disorder and osteoarticular disorder. Results from neurological disorder are numbness, tingling of hands and Carpal Tunnel Syndrome (CTS), an entrapment neuropathy (Joas et al., 2000), whereas osteoarticular disorder causes degenerative changes in bones and joints of the wrist and elbow (Bovenzi, 1998).

2.2 Standards for measurement and evaluation of hand-transmitted vibration

In the previous section, it has been highlighted that exposures to hand-transmitted vibration results in various disorders in hand-arm system. However, not all frequencies, magnitudes or durations of these exposures to hand-transmitted result in the same effects (Mansfield, 2005). In order to make the exposure data more comparable, they are measured using several standard procedures.

In 1986, the International Standard Organization (ISO) drew up the first guideline for the measurement and assessment of hand-transmitted vibration, named ISO 5349 (1986). However, this standard was replaced by the new version of ISO 5349 in 2001 (Mansfield, 2005). The current ISO 5349 (2001) is divided into two parts. The first part of the ISO 5349 (2001) provides the general requirement for measuring and reporting hand-transmitted vibration exposures. It also defines a frequency weighting filter, W_h which is the combination of band limiting and weighting filter, to allow uniform comparison of measurements (Figure 2.1). This filter forecast adverse effect of hand-transmitted vibration over the frequency range by the octave bands from $8 - 1000Hz$, and is based on the premise

that the low frequencies are considered to be most harmful. Frequencies outside this range are not considered. The vibration total value, a_{hv} is established by root-sum-of squares of frequency-weighted RMS acceleration measured in three orthogonal axes, written as (ISO 5349-1, 2001):

$$a_{hv} = \sqrt{a_{hwx}^2 + a_{hwy}^2 + a_{hwz}^2} \tag{2.1}$$

where a_{hwx}, a_{hwy}, a_{hwz} are the value of a_{hw} (frequency-weighted RMS acceleration in single axis) in metres per second squared, ms^{-2} , for the axes denoted x, y, z respectively.

Although the measurement on three axes simultaneously is the requirement of ISO 5349-1 (2001), when it is not possible to measure in all the axes, the estimate vibration total values can be obtained from single axis measurement using the estimation given in ISO 5349-2 (2001). Apart from the estimation of vibration total values, a_{hv} , the second part of the ISO 5349 (2001) has also listed the further guidance on the duration of measurement, mounting of accelerometer, and information to be reported.

Although the ISO 5349 (1986) has been replaced, it is discussed in this section, because there is much literature (Cherian et al, 1996; Chan & Yeh, 2000) which used this standard. According to Mansfield (2005), the ISO 5349 (1986) and ISO 5349 (2001) are generally the same (frequency weighting, methods), with two exceptions. The first exception is ISO 5349 (1986) was based on measurement on single dominant axis only. The other difference is that the old version of ISO 5349 used a reference period of 4 hours rather than 8 hours in new version of ISO 5349 for daily vibration exposure. Somehow, there can straight converse between each other with:

$$A(8) = A(4)/\sqrt{2} \tag{2.2}$$

where $A(8)$ and $A(4)$ are the daily vibration exposure based on reference periods of 8 hours and 4 hours respectively.

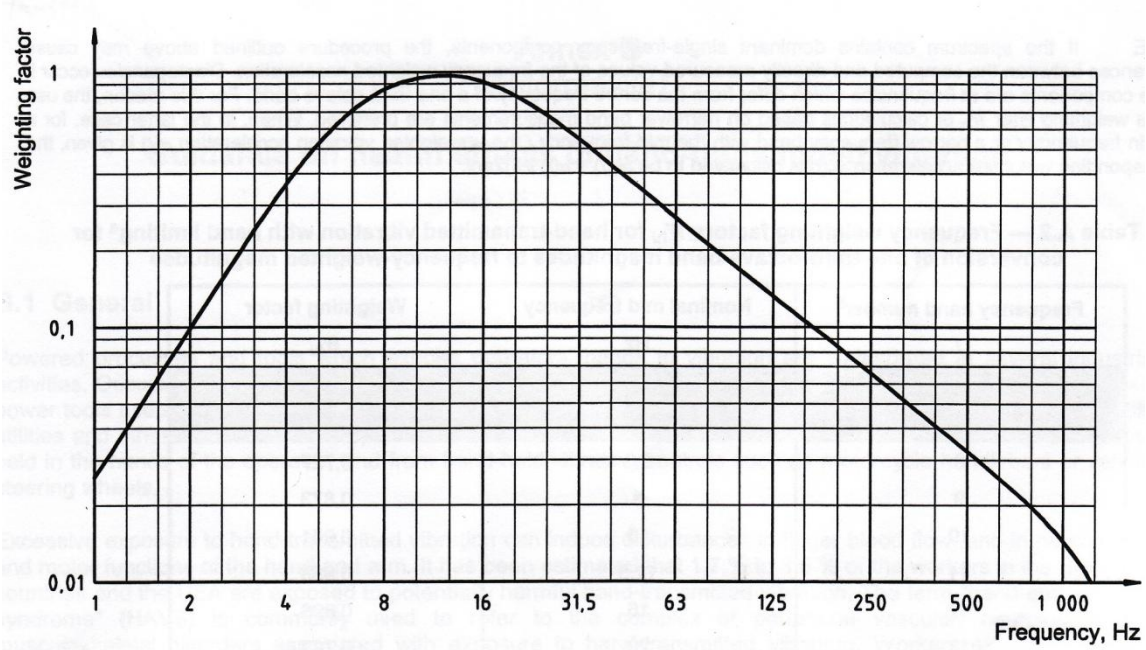

Figure 2.1: Frequency weighting filter, W_h for hand-transmitted vibration with band-limiting included (ISO 5349-1, 2001)

Although the ISO 5349 has standardized the measurements, it does not provide the dose-exposure relationship of hand-transmitted vibration. The European Union (EU) has adopted a directive in 2005, which provides the guidance for making risk assessments based on ISO 5349 (2001).

EU (2005) is the replacement of the earlier version of the standard which was established in 2002 (Nelson & Brereton, 2005; European Parliament and the Council of the European Union, 2005). The EU (2005) has set an exposure action value (EAV) of $2.5ms^{-2}$ and an exposure limit value (ELV) of $2.5ms^{-2}$ for daily vibration exposure, $A(8)$. The daily vibration exposure $A(8)$ is derived from vibration total value, a_{hv} and daily exposure duration, given as (ISO 5349-1, 2001):

$$A(8) = a_{hv}\sqrt{\frac{T}{T_0}} \tag{2.3}$$

where T is the total daily duration and T_0 is the reference duration of 8 hours. The employers are required to take action to control the hand-arm vibration risk of employee's workplace, if the daily vibration exposure, $A(8)$ is above the exposure action value. Meanwhile, the exposure limit value is the limit above which employees should not be exposed to.

2.3 Epidemiological study of hand-arm vibration

Millions of workers, who are involved in the operating of hand-held tools are exposed to hand-transmitted vibration (Thomas & Beauchamp, 1998). An epidemiological study in South Africa gold mines showed that 15% of the rock drill workers have been diagnosed with hand-arm vibration syndrome (HAVs). Among these 15% workers, 8% had both the vascular and neurological syndromes, 5% had only neurological syndrome and 2% had only vascular disorder (Sampson & Niekerk, 2003). This high level of HAVs is due to the weighted vibration levels of the rock drills which exceed $20ms^{-2}$ (Niekerk et al., 1998).

Bovenzi et al. (2005) investigated the prevalence of HAVs among the female workers using orbital sander. With the weighted RMS acceleration of orbital sander averaged from $3.7ms^{-2}$ to $7.3ms^{-2}$. 4% of 100 female workers had vascular disorder while 19% of them were diagnosed with CTS. Recently, another epidemiological study for the assessment of HAVs involving 26,842 workers in mining industry was carried out by Burke et al. (2005), where 15% of the workers were clinically assessed as having both HAVs and CTS.

Additionally other studies reported have investigated the contribution of exposure duration (Gerhardsson et al., 2005; Yamamoto, 2002), environmental variables (Scheffer et al., 1989; Yamamoto, 2002); and gender differences (Bylund, 2004; Neely et al., 2006) to the development of HAVs. Neely et al. (2006) concluded that there are no differences between male and female subjects for threshold measurement, while Bylund (2004) stated that both female and male are receiving the same power absorption.

2.4 Review on biodynamic models of human hand-arm

In order to evaluate the actual vibration response characteristic of human hand-arm system, different investigators have proposed different biodynamic models for human hand-arm system. These biodynamic models of human hand-arm are called biodynamics because they describe the dynamic behaviors, such as motion or force of the hand-arm system (Dong et al., 2005). The biodynamic response of human hand-arm play important roles for the measurement, evaluation, vibration-attenuation mechanisms, and risk assessment of hand-transmitted vibration exposure (Rakheja et al., 2002).

Based on the different characteristics of the biodynamic response, Rakheja et al. (2002) categorized these biodynamic models into two main groups: (1) to-the-hand-response, expressed in terms of driving-point of the hand-arm system; (2) through-the-hand-response, express the transmission of vibration to specific segment of hand-arm system.

2.4.1 To-the-hand biodynamic model

The biodynamic response characteristics of human hand-arm subject to vibration has been widely described in terms of driving-point mechanical impedance (DPMI), which is categorized in the first group. DPMI is conventionally defined as the complex ratio of applied excitation force, $F(j\omega)$ to the resulting vibration velocity, $\dot{X}(j\omega)$. It is expressed as:

$$Z(j\omega) = \frac{F(j\omega)}{\dot{X}(j\omega)} \tag{2.4}$$

Since it is a complex quantity, it possesses real and imaginary part, which can be calculated with the magnitude and phase. The measurement is usually carried out by measuring the input force, and the resulting velocity at the hand-handle interface.

Most of these proposed biodynamic models are lumped mass approximate models, only few are distributed parameter models. These models varied from single degree-

freedom-system to multi degrees-of-freedom-system and have been comprehensively reviewed by Rakheja et al. (2002).

In 1972, Reynold and Soedel developed a single DOF lumped-mass model for each of the three orthogonal axes. Five years later, Mishoes and Suggs (1977) proposed a 3-DOF hand-arm model. They also found that the hand was a highly damped system, with increasing acceleration and hand grip. In the following year, the first beam model was developed by Wood et al. (1978). This model used the distributed mass and stiffness parameters to represent each long bone of the arm as flexural beam. In 1979, Miwa et al. proposed a 2-DOF semi definite model of human hand-arm system as reported by Rakheja et al. (2002). Between 1982 and 1998, there are several 3-DOF and 4-DOF models reported by different investigators. These models were presented by Daikoku & Ishikawa, Reynolds & Falkenberg, Guram and ISO-10068 (Rakheja et al., 2002). The second beam model of hand-arm model has been reported in ISO 10068 (1998).

There are significant differences for the parameters of these to-the-hand biodynamic hand-arm models (Dong et al.,2005; Gurram & Rakheja, 1995). According to Rakheja et al. (2002), these differences were due to two factors: (1) the investigators used different test conditions (grip force, vibration level, frequency range type of excitation, posture) during DPMI measurements; (2) the measurement methods have not been standardized. Owing to the variety of the kinds of models reported, Rakheja et al. (2002) studied and compared these entire to-the-hand models to evaluate their suitability for the application to coupled hand tool. They concluded that most of the models are not suitable for development of mechanical-simulator or the assessment of dynamic behaviors of the coupled hand-tool system. The main reason for the higher degrees of models not suitable for the laboratory mechanical-simulator was due to these models using very light masses (1-8g). Furthermore, low-degrees models are not suitable for assessment of dynamic behaviors of coupled hand-tool system since these models do not satisfy the recommended DPMI response as reported in ISO 10068.

ISO 10068 reported three DPMI hand-arm models in 1998, however the reliability of those models are questionable (Rakheja et al., 2002). The ISO 10068 beam model can result in positive eigen value which causes instability. Meanwhile, the ISO 10068 4-DOF model has relatively high damping ratio and the exhibit modes did not coincide in the formulated frequency range of $10 - 500Hz$ (Rakheja et al., 2002). For the ISO 10068 3-DOF model, although the modes are inside the formulated frequency range of $10 - 500Hz$, Adewusi et al. (2007) concluded that this model characterize the bone structure of human hand-arm model only but not the muscle structure. Thus, it does not fully represent the characteristic of human hand-arm model.

There are a great number of studies related to the driving-point dynamic response. However, the majority of these studies looked into the influence of biodynamic factors, such as vibration direction, type of vibration, hand-arm posture, handle size, muscle tension, grip and feed force on the mechanical impedance of human hand-arm, (Besa et al., 2007; Burström, 1997; Aldien, 2006; Dong et al., 2004; Dong et al., 2005; Kihlberg, 1995; Aldien, 2005; Marcotte, 2005). Only few studies have reported the application of DPMI or to-the-hand biodynamic model to assess the dynamic behavior of coupled hand-tool systems.

Oddo et al. (2004) applied the ISO 10068 second model (4 DOF) coupled with suspended handle, to study the effectiveness of the mitigation to attenuate vibration transmitted to hand. They found that this model characterize the biodynamic response of human hand-arm fairly well, when validated with two male subjects. Besides, the 4-DOF hand-arm model proposed by Rakheja et al. in 1984 has been used by Kadam, 2006 in his master's study. He studied the vibration characterization numerically and experimentally of this model when coupled with a pneumatic impact hammer. He found that the models cannot be used to set up experimental hand-arm rig since the masses used in the model are extremely small, which is similar to the observations by Rakheja et al. (2002).

2.4.2 Through-the-hand biodynamic model

The second type of biodynamic model is derived in terms of transmissibility, which is defined as a complex non-dimensional ratio of the resulting motion to the forcing motion. The ratio may be in the form of displacement, velocity or acceleration, expressed as:

$$T(j\omega) = \frac{X_o}{X_i}(j\omega) = \frac{\dot{X}_o}{\dot{X}_i}(j\omega) = \frac{\ddot{X}_o}{\ddot{X}_i}(j\omega) \tag{2.5}$$

where $T(j\omega)$ is the complex vibration transmissibility, $X_0(j\omega)$, $\dot{X}_0(j\omega)$, $\ddot{X}_0(j\omega)$ are the resulting displacement, velocity, and acceleration complex response due to the forcing displacement, velocity and acceleration excitation $X_i(j\omega)$, $\dot{X}_i(j\omega)$, $\ddot{X}_i(j\omega)$ respectively.

There are only a small number of studies, namely Reynold & Angevine (1977), Cherian et al. (1996), Fritz (1991) and Gurram (1993) using through-the-hand biodynamic response (Rakheja, 2002; Cherian et al., 1996). According to Cherian et al. (1996), this trend may be due to the insufficient reliable vibration transmissibility data and complexities of parameter identification.

Cherian et al. (1996) contributes to model development based on vibration transmissibility or though-the-hand response. They proposed a five DOF biomechanical model, which represents the viscoelastic and inertia properties of human hand-arm. The parameters of this model are obtained from the anthropometric data and characteristics of vibration transmitted to hand, forearm and upper arm. Furthermore, they also analytically evaluated the effect of the coupled flow divider and hand-arm model to attenuated hand-transmitted vibration. In addition, the attenuation effect of the flow divider on the forearm and upper arm were also reported.

Hand-transmitted vibration has a strong influence on hand-arm vibration syndrome (Cherian et al., 1996). Hence it is important to study the vibration transmitted characteristics to the hand and to the arm. Since measurement on this type of biodynamic response is

carried out by measuring the vibration (acceleration) on the human hand-arm system and the input vibration (Dong, 2005), it fully express the characteristic of vibration transmitted to the segment of the hand-arm system. This measurement has the advantage that it can be obtained mostly directly from the signals provided from accelerometers.

2.5 Mitigation of hand-transmitted vibration

Over the past two decades, there have been great efforts made by researchers in order to protect operators of hand-held tools from hand-transmitted vibration. Commonly, these techniques can be classified based into three principles: (1) control the vibration from source (hand-held tool); (2) vibration attenuation or dynamic absorption of vibration; (3) isolate the vibration from the hand-grip interface (Golysheva, 2004).

2.5.1 Control of vibration from the source

This first design principle might be the best choice in vibration reduction, but it is the least used by researchers. Usually, it involves redesign of the tools, which can be costly and complex. Tudor et al. (1996) redesigned an ergonomic handle for a string trimmer. The newly designed handle is curve shaped, with a foam surface to increase the friction force at hand-handle interface. The redesigned handle not only successfully reduces vibration but also improves the operator comfort and reduce fatigue. A study by Greenslade and Larsson, (1999) showed that the chainsaws used by Finnish lumberjacks where redesigned result significantly reduces in vibration levels from $14ms^{-2}$ to $2ms^{-2}$ (Dias & Sampson, 2005).

2.5.2 Dynamic absorption on vibration

The second method of reducing vibration can be achieved by increasing the secondary mass or inertia (Golysheva, 2004), such as by adding a dynamic vibration absorber on the source or receiver. Strydom (2000) designed a dynamic vibration absorber mounted on the handle of rock drill. The vibration absorber was tuned so that it coincides

with the operating frequency of the rock drill. The attenuated handle has reduce the displacement acceleration about 20% to 40%. However, he has stated that the vibration absorber required additional mass in order to tune the isolation frequency to typical drill operating frequencies.

Cherian et al. (1996) introduced a vibration absorption on the receiver. They proposed a 0.5 kg flow divider attached to a 5 DOF hand-arm model. The overall weighted acceleration of the hand decreased by 22%, while the forearm and the upper arm increases by 13% and 10% respectively (Cherian et al., 1996). This is due to the characteristic of dynamic vibration absorber. Although it tends to absorb vibration at the connection point, it increases vibration in some other points (Steffen & Rade, 2002).

2.5.3 Isolate the vibration from the hand-grip interface

The hand-arm vibration level can also be reduced by placing an isolator between hand and handle. These types of isolation are made of elastomeric, rubber like or foam material.

The anti-vibration glove used to isolate vibration transmitted to hand is one example of vibration isolation system made of elastomeric material. Several studies of evaluating the effectiveness of anti-vibration gloves have been carried out (Chang et al., 1999; Dong et al., 2003). Commercial anti-vibration glove are available in the market, but most of them are only effective at frequencies above $100\,Hz$ (Sampson & Niekerk, 2003). Since the anti-vibration glove is location specific, the glove may reduce the vibration level significantly at the palm, but insignificantly at the fingers (Dong et al., 2005). Besides, individual factors (Dong, et.al 2005) and tool-specific factors (Rakheja, et.al, 2002) are directly associated with the effectiveness of anti-vibration gloves. In additional, thick glove may cause inconvenience

while grasping the tools and excessive wearing may cause skin problem (Sampson & Niekerk, 2003).

The use of vibration isolation, especially made of elastomeric material, to reduce vibration transmissibility in structures is well known. Elastomeric materials have been used as anti-vibration glove, vibration isolators in motors, engines and suspended handles (Dimarogonas, 1996; Oddo, 2004).

2.6 Discussion

From this review, it is clear that the use of hand-held power tools can result in hand-arm vibration syndrome (HAVs). The use of orbital sanders can produce high level in weighted RMS acceleration of $6.8ms^{-2}$ as reported by Cherian et al. (1996) and $3.7ms^{-2}$ to $7.3ms^{-2}$ (Bovenzi et al., 2005).

The mitigation effects of the use of flow divider manage to bring down the overall weighted RMS acceleration at the hand from $6.8ms^{-2}$ to $5.3ms^{-2}$ (Cherian et al., 1996). However, no study has been made on the effect of elastomeric pad to reduce vibration level on human hand-arm. Anti-vibration gloves have been reported effective but only above $100Hz$ (Chang et al., 1999; Dong et al., 2003). When compared to the operating frequency of the orbital sander, the running speed has been increased from $8000\,rpm$ to currently $12{,}000\,rpm$ (available in the market). This translates to operating frequencies of approximately $125\,Hz$ to $228\,Hz$ which may be suitable for anti-vibration glove. However, the use of the glove is not recommended for prolonged use since it may cause skin problems (Sampson & Niekerk, 2003) and inconvenience.

This work therefore will use the elastomeric pad in a way to reduce hand-transmitted vibration. To evaluate the effect of elastomeric pad on human hand-arm system, the coupled elastomeric pad and hand-arm model will be developed.

From the review of Rakheja et al. (2002), it is shown that the DPMI hand-arm model did not resemble human hand-arm closely enough for direct interpretation of the response. This is made worse by the fact that the identified model parameters using DPMI do not represent a unique solution with possible vast number of model parameters. Additionally, the ISO 10068 beam model is incapable of identifying the natural frequencies and damping ratio while the modes of ISO 10068 4-DOF model did not coincide with its formulated frequency range (Rakheja et al., 2002). Meanwhile, the ISO 10068 3-DOF model did not fully represent the characteristic of human hand-arm model (Adewusi et al., 2007).

Hence, in this study, the through-the-hand model proposed by Cherian et al. (1996) is adopted as the reference model. This model was selected due to the capability of representation the vibration transmissibility characteristic of human hand-arm system and because the model components corresponding to the hand-arm segments which related to the anthropometric data.

CHAPTER 3
METHODOLOGY

3.0 Overview

In this chapter, the explanations of comparing the overall weighted RMS acceleration of hand-arm model, hand-arm model with flow divider and hand-arm model with elastomeric pad are presented. Subsequently, the methodologies used to determine the new hand-arm parameters, calculation of the anthropometric data, and the input spectrum from experiment are presented. The analytical studies of the effect of elastomeric pad for attenuating hand-transmitted vibration are also explained and the experimental set up to verify the analytical work is clarified. Finally, the calculation of daily vibration exposure, $A(8)$ is presented. In short, the main topics discussed in this chapter are:

- Comparison of the effect of elastomeric pad on the hand-arm model with Cherian's work
- Analytical investigation on the effect of elastomeric pad to attenuate hand-transmitted vibration when subjected to $12{,}000\ rpm$ input spectrum
- Experimental verification
- Determination of A(8)

3.1 Comparison of the effect of elastomeric pad on the hand-arm model with Cherian's work

The five DOF hand-arm model proposed by Cherian et al. (1996) was selected as the study model. For the first step, in order to compare the effect of elastomeric pad on human hand-arm model with the concept of flow divider (Appendix A) reported by Cherian et al. (1996), methodologies to deliver the RMS acceleration response spectrum of human hand-arm model, coupled elastomeric pad and hand-arm model, are presented in Section 3.1.1 and 3.1.2 respectively. The way for the comparison in terms of overall weighted RMS acceleration is clarified in Section 3.1.3.

3.1.1 Five DOF hand-arm model

Schematic of the selected five DOF hand-arm model is illustrated in Figure 3.1. This hand-arm model is designed to be active in the longitudinal direction (z-direction). $m_1, m_2,$ m_3 represent the hand, forearm and upper arm masses respectively. In addition, the upper arm mass, m_3 is presumed to undergo motion in three directions: longitudinal (z-direction), vertical (x-direction), and pitch (θ) due to rotational at the shoulder and elbow joints. Z_1 , Z_2 , Z_3 represent the longitudinal motions of masses hand, forearm, upper arm respectively. Meanwhile, θ_3 characterizes pitch rotation of the upper arm with respect to the elbow joint; X_3 represents vertical motion of the elbow joint with respect to the longitudinal axis passing through the forearm. The stiffness and damping properties at the hand-handle interface are characterized by K_0 and C_0. (K_1, C_1) are the viscoelastic properties of the hand and forearm at wrist joint, while (K_2, C_2) represent the viscoelastic properties of forearm at elbow joint. (K_3, C_3) are the viscoelastic behavior of upper arm at shoulder joint in the longitudinal direction. This is similar with (K_4, C_4), except it is in vertical direction. Meanwhile, (K_{t2}, C_{t2}) and (K_{t1}, C_{t1}) show the viscoelastic properties in the pitch direction of forearm at elbow joint, and upper arm at shoulder joint respectively. L is the length of upper arm and L_{cg} is the distance between the elbow and the centre of gravity of the upper arm, whereas, γ shows the angle of upper arm.

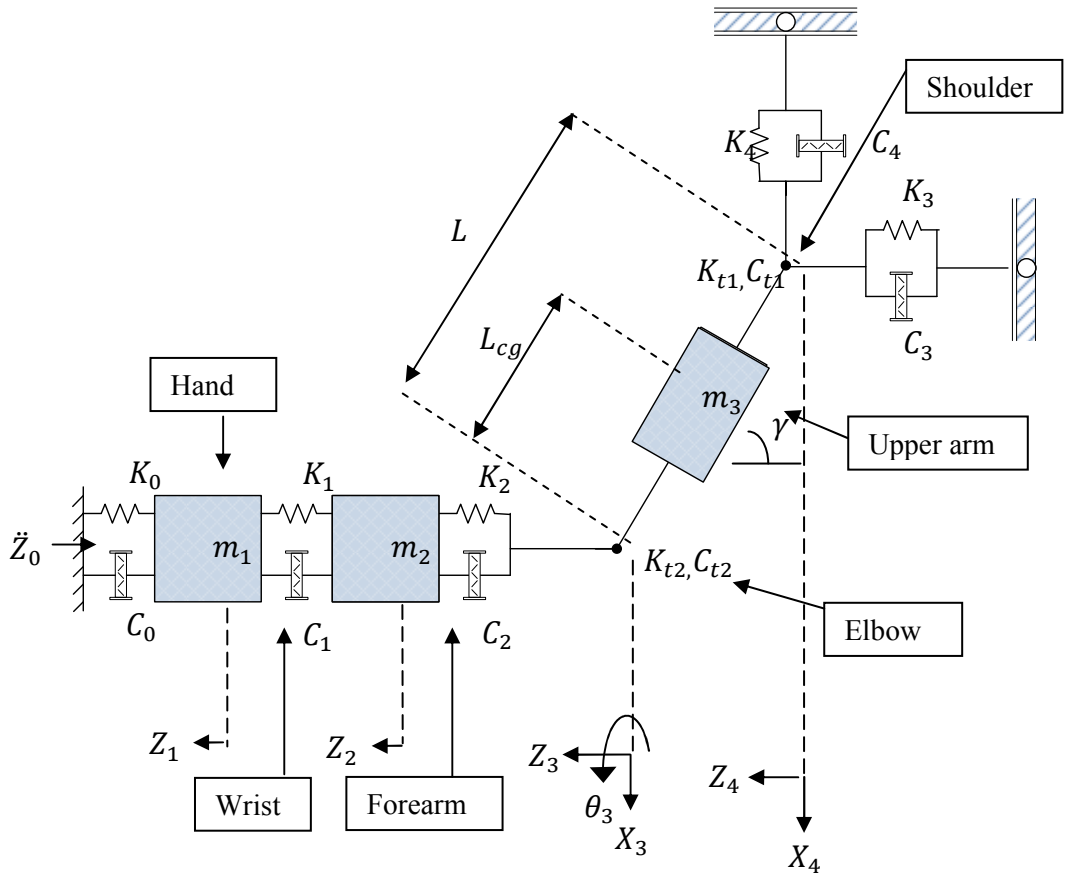

Figure 3.1: Diagram of the five DOF hand-arm vibration model in the z-direction (Cherian et al., 1996).

3.1.1.1 Form the equation of motion of human hand-arm model

Based on Newton's second law, the equation of motion of this five DOF hand-arm model when subjected to base excitation (longitudinal acceleration,$\ddot{Z}_0$) is as below:

$$[M]\{\ddot{U}\} + [C]\{\dot{U}\} + [K]\{U\} = \{K_i\}Z_0 + \{C_i\}\dot{Z}_0 \tag{3.1}$$

where$[M]$ represents the 5×5 mass matrix, $[C]$ is the 5×5 damping matrix, $[K]$ shows the 5×5 stiffness matrix. $\{C_i\}$ and $\{K_i\}$ are the forcing damping andstiffness vectors. Meanwhile, $\{U\}$ represents (5×1) vector of generalized displacement coordinates, given as:

$$\{U\} = \begin{bmatrix} Z_1 \\ Z_2 \\ Z_3 \\ X_3 \\ \theta_3 \end{bmatrix} \tag{3.2}$$

3.1.1.2 Hand-arm system response spectrum

Using the model parameters reported by Cherian et al. (1996), shown in Table 3.1, the RMS acceleration response spectrum of hand-arm system is evaluated using:

$$\{S_o(\omega)\} = \left\{\left|\frac{\ddot{U}}{\ddot{Z}_0}(j\omega)\right|\right\} S_h(\omega) \tag{3.3}$$

where $\frac{\ddot{U}}{\ddot{Z}_0}(j\omega)$ is the complex acceleration transmissibility function of hand-arm model, evaluated from Fourier transform of Equation 3.1, given as:

$$\frac{\ddot{U}}{\ddot{Z}_0}(j\omega) = \left[[K] - \omega^2[M] + j\omega[C]\right]^{-1} \times [\{K_i\} + j\omega\{C_i\}] \tag{3.4}$$

where $\ddot{Z}_0$ represents the amplitude of acceleration excitation, $\{\ddot{U}\}$ is the complex amplitude vector of acceleration response at the hand, forearm and upper arm. The complex acceleration transmissibility response function for hand $\left[\frac{\ddot{U}_1}{\ddot{Z}_0}(j\omega)\right]$, forearm $\left[\frac{\ddot{U}_2}{\ddot{Z}_0}(j\omega)\right]$, and upper arm $\left[\frac{\ddot{U}_3}{\ddot{Z}_0}(j\omega)\right]$, can then be derived from Equation 3.4. Meanwhile, in order to directly compare with Cherian et al.'s work, the RMS acceleration input spectrum for an orbital sander, $S_h(\omega)$ with $8000\ rpm$ are used.

Table 3.1: Parameters of biomechanical model as reported by Cherian et al. (1996)

$m_1 = 0.45kg$	$K_0 = 155.8kN/m$	$C_0 = 30Ns/m$	$L = 0.298m$
$m_2 = 1.15kg$	$K_1 = 23.6kN/m$	$C_1 = 202.8\ Ns/m$	$L_{cg} = 0.1788m$
$m_3 = 1.90kg$	$K_2 = 444.6kN/m$	$C_2 = 500Ns/m$	$J_c = 0.0149kgm^2$
	$K_3 = 415.4kN/m$	$C_3 = 164.6Ns/m$	$\gamma = 90^\circ$
	$K_4 = 50.25kN/m$	$C_4 = 50Ns/m$	
	$K_{t1} = 2Nm/rad$	$C_{t1} = 6.14Nms/rad$	
	$K_{t2} = 2Nm/rad$	$C_{t2} = 4.9Nms/rad$	

3.1.2 Development of the coupled elastomeric pad and five-DOF hand-arm model

In this section, the elastomeric pad model is introduced into the chosen hand-arm model. The coupled elastomeric pad and five DOF hand-arm model is illustrated in Figure

3.2. It is similar with Figure 3.1, except there is an additional Kelvin-Voigt elastomeric pad model.

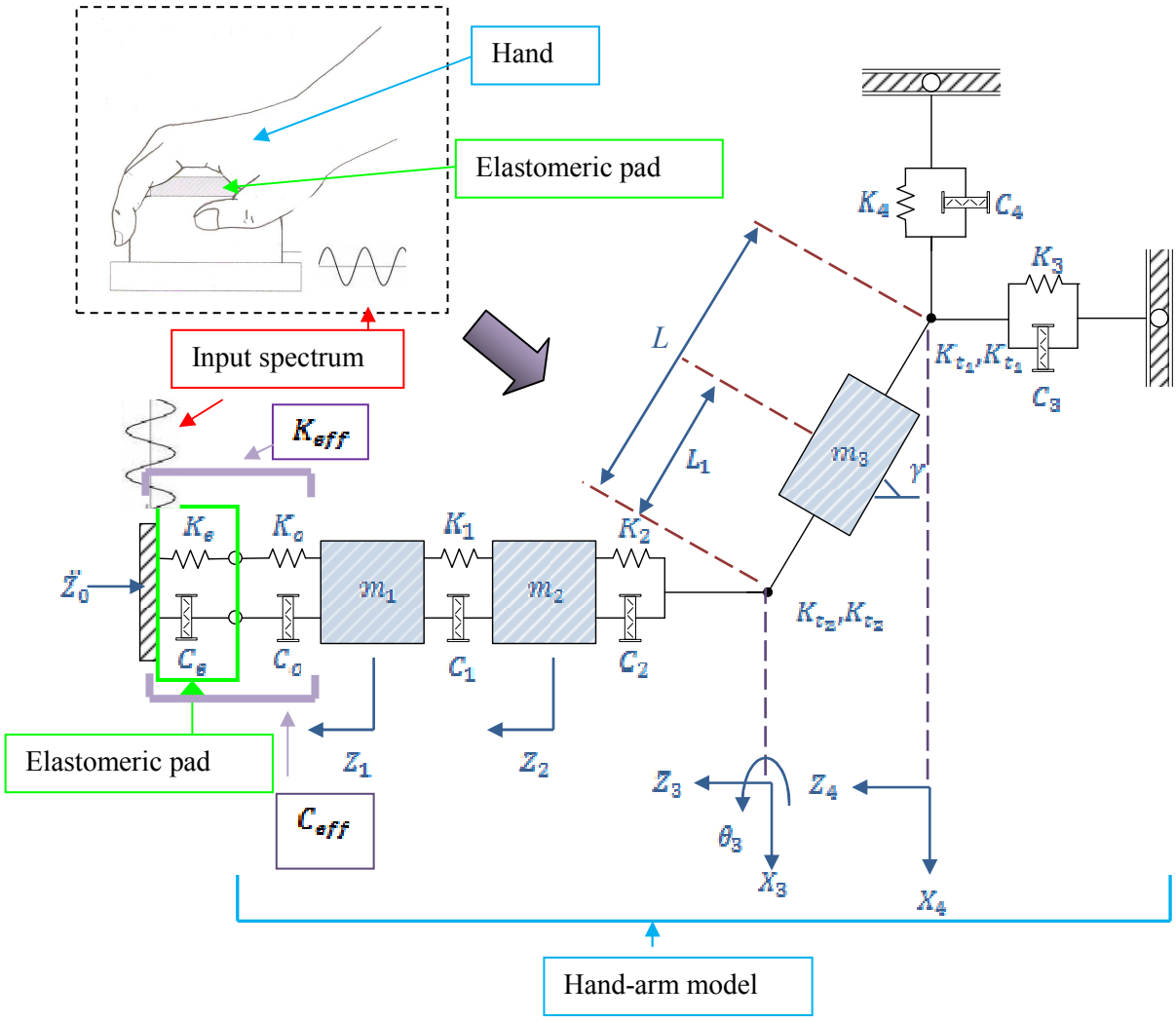

Figure 3.2: Representation of coupled elastomeric pad and hand-arm model

3.1.2.1 Properties of elastomeric pad

The elastomeric pad has both stiffness and damping properties. This can be represented by the familiar mass-less Kelvin-Voigt model, which consists of a spring and a viscous damper (Yunhe et. al, 2001) as shown in Figure 3.3.

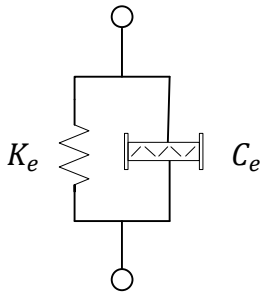

Figure 3.3: Kelvin-Voigt type of elastomeric pad

In terms of the complex modulus of elasticity, the damping, C_e is due to the viscoelastic behavior of stiffness, is represented by:

$$C_e = \frac{\eta K_e}{\omega} \tag{3.5}$$

where K_e is the stiffness of elastomeric pad, η is the elastomeric pad's loss factor, and ω is the excitation frequency (Dimarogonas, 1996).

3.1.2.1 (a) Determination of damping behavior of elastomeric pad

For the purpose of determination of the loss factor, η of the elastomeric pad, logarithmic decrement technique can be used. The test set up consisted of a test specimen, impulse force hammer (*Kistler, type: 9724A5000*), an accelerometer (*Kistler, type: 8776A50*), analyzer *(IMC cs-8008)*, as shown in Figure 3.4. The schematic diagram of the test specimen is shown in Figure 3.5. The impulse hammer is used to excite the test specimen under free damped vibration. The signals captured from the accelerometer is transmitted to the analyzer, and then used in a computer program, *IMC wave* for data processing. The loss factor of elastomeric pad can then be evaluated from the envelope of the damped sinusoidal response (Cortés & Castillo, 2006, Huang et al., 2007). Details for the logarithmic decrement technique are discussed in Appendix B.